Journal Pre-proof

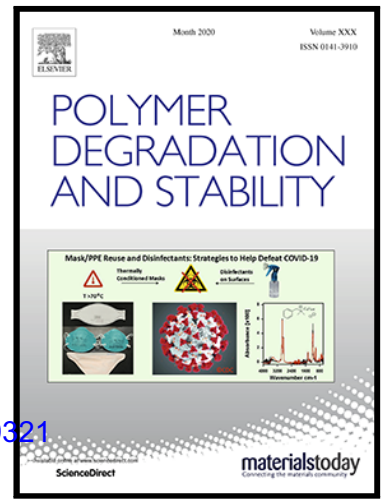

EFFECT OF PROCESSING TEMPERATURE AND MIXING TIME ON THE PROPERTIES OF PP/GnP NANOCOMPOSITES

Luigi Botta , Francesco Paolo La Mantia , Manuela Ceraulo , Maria Chiara Mistretta

PII: S0141-3910(20)30252-4
DOI: https://doi.org/10.1016/j.polymdegradstab.2020.109321
Reference: PDST 109321

To appear in: *Polymer Degradation and Stability*

Received date: 30 May 2020
Revised date: 5 August 2020
Accepted date: 8 August 2020

Please cite this article as: Luigi Botta , Francesco Paolo La Mantia , Manuela Ceraulo , Maria Chiara Mistretta , EFFECT OF PROCESSING TEMPERATURE AND MIXING TIME ON THE PROPERTIES OF PP/GnP NANOCOMPOSITES, *Polymer Degradation and Stability* (2020), doi: https://doi.org/10.1016/j.polymdegradstab.2020.109321

Highlights

- The effect of mixing conditions on properties of PP/GnP nanocomposites was evaluated
- Graphene nanoplatelets improve the thermo-mechanical resistance of the matrix
- The sample with the lower content of GnP exhibits a lower level of thermo-mechanical degradation

EFFECT OF PROCESSING TEMPERATURE AND MIXING TIME ON THE PROPERTIES OF PP/GnP NANOCOMPOSITES

Luigi Botta[a], Francesco Paolo La Mantia[a,*], Manuela Ceraulo [b], Maria Chiara Mistretta [a]

[a] Dipartimento di Ingegneria, UdR INSTM di Palermo, Università degli Studi di Palermo, Viale delle Scienze, 90128 Palermo, Italy
[b] INSTM, Via Giusti 9, 51121, Firenze (Italy)

ABSTRACT

During processing of molten polymers the thermal and mechanical stress acting on the melt in presence of oxygen can induce degradation with a modification of the chemical structure of the polymers. This picture can become even more relevant if the melt is a multiphasic polymer system. In this last case, the effects of the degradation depend also on the presence of a second phase and on the interactions between the two phases.

In this work, the effect of the processing conditions, temperature and time, have been considered in order to investigate the thermo-mechanical and thermo-oxidative degradation of nanocomposites made by polypropylene and different contents of graphene nanoplatelets. Graphene nanoplatelets improve the stability of the polymer matrix and the sample with the lower content of nanofiller shows a lower level of degradation. The better resistance of the filled samples has been interpreted with a barrier effect to the oxygen of the nanofiller that hinders the transport of oxygen necessary for the oxidation of the polypropylene. The unexpected effect of the concentration of graphene nanoplatelets has been correlated with the agglomeration of the nanoplatelets that reduces the surface area of the filler and then the barrier effect to the oxygen.

Keywords: Nanocomposites; Graphene nanoplatelets (GnP); Polypropylene; thermo-mechanical degradation

INTRODUCTION

Among the many nanoparticles studied in recent decades, carbonaceous nanofillers have attracted a great interest from both an industrial and a scientific point of view because of their unusual and extraordinary physical properties. The peculiar chemical structure and huge aspect ratio of these carbonaceous particles impart very relevant thermal, mechanical, and electrical properties, exhibiting great potentials in applications, such as electrochemical devices, hydrogen storage and nanocomposites.

Graphene Nanoplatelets (GnP), recently developed, are short stacks of individual layers of graphite that often increase the tensile modulus of a composite material and are available at a low cost [1–5].

One of the most promising applications of GnP is their use in formulation of polymer-based nanocomposites[6–14]. The addition of GnP, even at low filler concentration (< 5 wt. %), can lead to the enhancing of the thermal, heat-resistance, mechanical and electrical properties of the polymer matrix due to both unique properties of these nanofillers and their exceptionally large specific surface area. Many researches have shown that the influence of these nanoparticles on the properties of this class of polymer based nanocomposites is of course related to a good dispersion achieved during processing and good adhesion of the filler within the matrix [15–18]. However, in many cases the huge surface area, the incompatibility with the polymer matrix did not always allow obtaining the expected reinforcement of the matrix because good dispersion and good adhesion are not easy to obtain.

The effect of the processing conditions on the morphology and the final properties of nanocomposites has been studied by our research group [12,19–27] and the obtained results suggest that the thermo-mechanical stress and the processing time are effective to alter the morphology of the nanocomposites made with both organomodified clay and carbon nanotubes, being able to align the nanofillers along the flow direction but also to modify the degradation kinetics of the nanocoposites in comparison with the pure matrix.

Although some papers [28–32] have investigated the improved thermal stability of GnP based nanocomposites, to our best knowledge, no scientific papers are reported in the literature concerning the possible thermo-mechanical and thermo-oxidative degradation during the preparation of the nanocomposites or during the processing necessary to obtain the manufactures. In this work polypropylene (PP) based nanocomposites with graphene nanoplatelets were prepared in different mixing conditions and their properties were investigated. In particular, the effect of mixing time and processing temperature on rheological and mechanical properties of PP/GnP

nanocomposites was evaluated and correlated with the achieved morphology. Furthermore, the effect of the GnP content on the evaluated properties was studied.

EXPERIMENTAL

Materials

The polymeric matrix used in this work is a sample of a polypropylene (PP) supplied by Carmel Olefins with trade name Capilene® E 50 E (M.F.I. = 1.8 g/10 min. at 230 °C/2.16 Kg).

Graphene nanoplatelets (GnP) were supplied by XG Sciences Inc. (Lansing, MI, USA) with trade name xGnP®, Grade C. According to the manufacturer, the main characteristics of the GnP used in this work are the following: average diameter between 1 and 2 µm; average thickness lower than 2 nm and a specific surface area of about 750 m^2/g. Production of this GnP grade is based on exfoliation of sulphuric acid-based intercalated graphite by rapid microwave heating, followed by ultrasonic treatment [33].

Preparation

GnP were added to PP pellets at 1 and 2 wt% at the solid state, and then the mixtures have been melt compounded in a batch mixer (Brabender Plasticorder PLE330) at 210 and 240 °C and a rotational speed of 60 rpm for times ranging from 5 to 60 min. For comparison, pristine polymer matrix was processed under the same conditions. Although the highest processing times are unrealistic for industrial processing, the tests were carried out in order to better investigate the effects of this parameter on the degradation of all the systems.

The processing conditions and the sample codes are reported in Tab. 1

Tab. 1 Samples codes and processing conditions of all the samples.

Sample code	Composition, %	Mixing temperature, °C
PP/210	PP 100	210
PP/240	PP 100	240
PP1/210	PP 99/GnP 1	210
PP1/240	PP 99/GnP 1	240
PP2/210	PP 98/GnP 2	210
PP2/240	PP 98/GnP 2	240

The specimens for the characterizations were obtained by compression moulding using a laboratory press (Carver, USA), operating at 210 °C.

Characterization

The morphology of the samples was observed by using both scanning electron microscopy (SEM; Quanta 200 ESEM, FEI, Hillsboro, OR, USA) and transmission electron microscopy (TEM; JEM-2100, JEOL, Tokyo, Japan). In particular, the samples for SEM analyses were fractured under liquid nitrogen and then glued onto the sample holder. All the samples were sputter coated with a thin layer of gold under argon atmosphere for 120 s (Scancoat Six Edwards, Crawley, UK) in order to avoid electrostatic charging under the electron beam.

TEM observations were performed on ultrathin films with a thickness of about 100 nm prepared via cutting from the epoxy block with a Leica (Solms, Germany) Ultramicrotome EM-UC6. Ultrathin slides of the samples were mounted on the lacey carbon films on 300 mesh copper grids and were then observed under an accelerated voltage of 200 kV.

The rheological measurements were performed on samples obtained by compression moulding by using a plate-plate rotational rheometer (HAAKE MARS, Thermo Scientific, Waltham, MA, USA), operating at 210 °C in air atmosphere. The instrument has been set to operate in the frequency sweep mode in the range 0.1-500 rad/sec with a strain of 5%. The tests were performed in triplicate.

FT-IR ATR spectra were collected by using a Perkin-Elmer (USA) Spectrum One spectrometer. Measurements were obtained from the average of triplicate samples and the spectra were measured with an average of 16 scans for each specimen.

Tensile tests were carried out by using a Universal Testing Machine (Instron model 3365, High Wycombe, UK) on rectangular shaped specimens (10×90 mm) cut off from sheets (thickness about 0.6 mm) prepared by compression moulding according ASTM D882 standard. The distance between the grips was 30 mm and the initial crosshead speed was 1 mm/min until the displacement achieved 2 mm. Thereafter the crosshead speed was increased to 100 mm/min until break. At least 8 specimens were tested for each material.

Thermal properties of the materials were investigated by a differential scanning calorimeter (Perkin Elmer DSC 7, USA). The experiments were performed under N_2 gas flow (20 mL/min). Samples underwent a heating/cooling/ heating program in the temperature range 30– 220°C. The scanning speed was 10 °C/min both for heating and for cooling. The experiments were performed in triplicate.

The crystallinity (χ) of PP and its nanocomposites was calculated by Equation (1):

$$\chi = \frac{\Delta H_m}{\Delta H_m^o} \cdot 100 \qquad 1)$$

where ΔH_m is the melting enthalpy of the sample and ΔH_m^0 is the melting enthalpy of 100% crystalline PP (209 J/g) [34].

Enthalpy values found for nanocomposites were normalized on the actual amount of polymer involved in the thermal transition, being GnP not involved in melting/crystallization processes.

RESULTS AND DISCUSSION

In Fig.1 the dimensionless curves of the torque as a function of the mixing time for all the investigated samples have been reported. The dimensionless values have been calculated by dividing the value of the torque at each time by that of the torque at 5 min to reach a thermal equilibrium and to eliminate the possible effects of the loading.

The torque curves decreases with time and this suggests that some degradation occurs during the mixing. Indeed, as already reported in literature [35] the torque lowering observed for PP indicates a lower shear resistance, indicating a higher fluidity caused by chain scission and consequent lowering of the molecular weight because of thermo-mechanical and thermo-oxidative degradative phenomena occurring during the compounding.

This reduction of the torque is more relevant at the highest temperature for the pure matrix, whereas for the nanocomposites the two curves are very similar and, rather, the reduction seems slightly more pronounced at the lowest temperature. Moreover, some stabilizing effect seems occur in presence of GnP, because the decrease of the curves of the torque is much less pronounced for both the two nanocomposites. However, this effect is more relevant for the sample with 1% of GnP. Moreover, it is important outline that during the compounding the morphology of nanocomposites can change and, as reported in literature for similar systems, longer mixing times can lead to improving level of particle dispersion and decrease the presence of aggregates [10] .

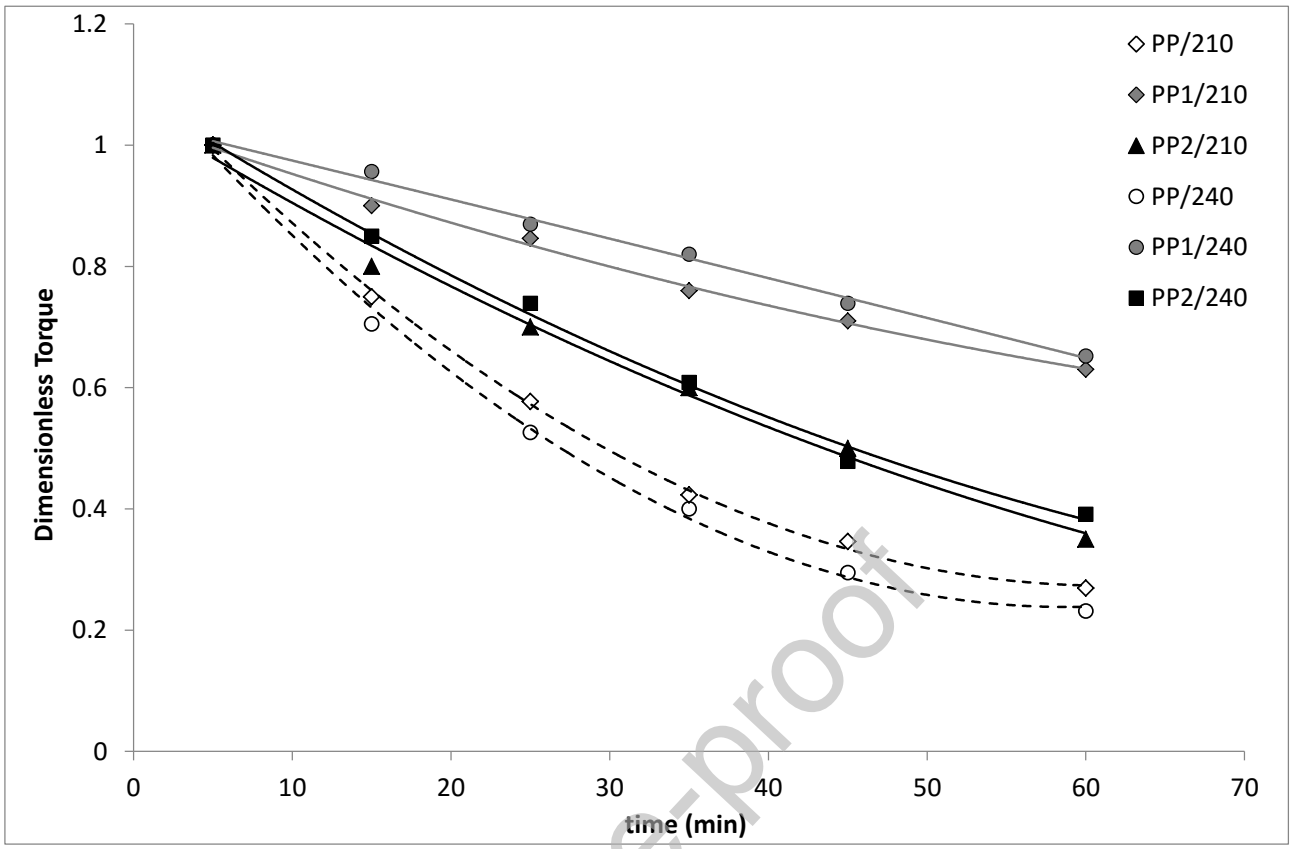

Fig.1 Dimensionless curves of the torque as a function of the mixing time for all the investigated samples.

To better put in evidence the effect of the GnP on the degradative behaviour of the PP, in Fig. 2 the data of the dimensionless torque curves reported in Fig. 1 has been divided by those of the PP matrix at the same temperature. These new dimensionless torque curves, then, put in evidence only the effect of the GnP on degradative behaviour. All the curves show values larger than 1 and this highlights the stabilizing effect of the GnP. The comments reported before are magnified and better put in evidence by these curves. Indeed, it is evident that the beneficial effect of the presence of the GnP occurs at the lowest content and at the highest temperature.

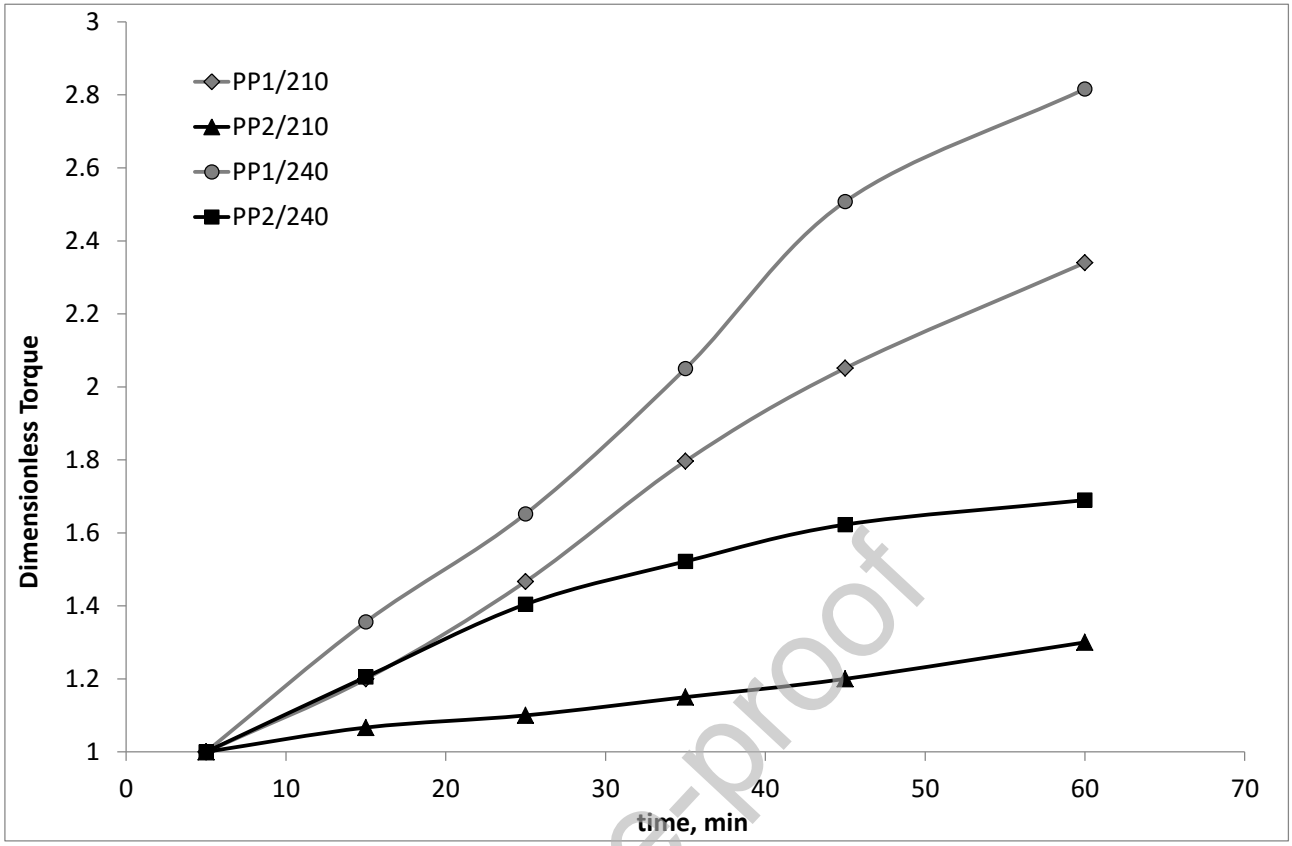

Fig. 2 Dimensionless torque curves as a function of the mixing time of the nanocomposite samples divided that of the matrix.

The change of the molecular weight, due to the degradative phenomena, can be easily observed by the Newtonian viscosity because this property is strongly dependent on the molecular weight for the pure polymer. Moreover, the Newtonian viscosity of the nanocomposites, is also dependent on shape and size of the nanoparticles and on their distribution. The flow curves of PP1 and PP2 samples processed for 5 and 60 min at 210 °C are reported in the Figs. 3. The curves relative to the PP matrix subjected to the same treatment are also reported.

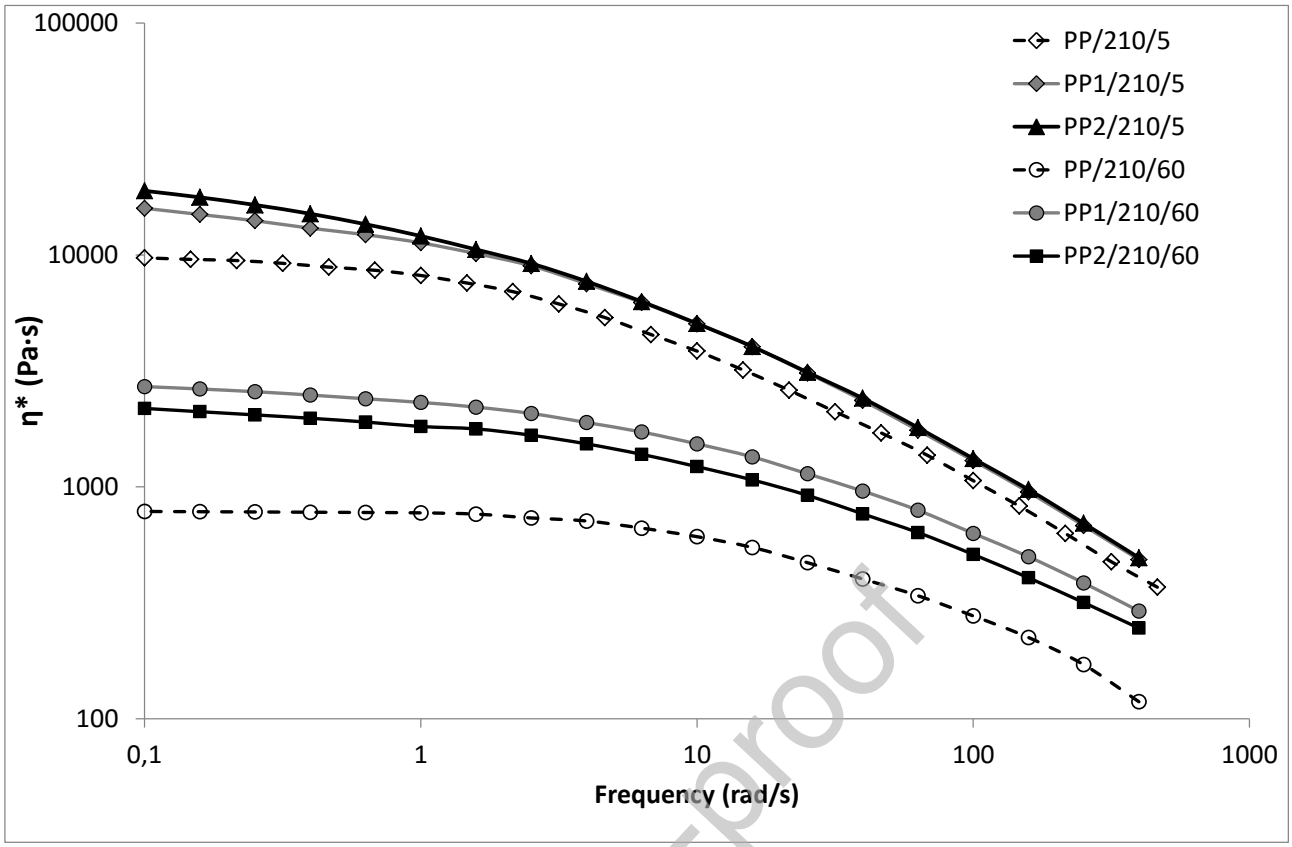

Fig. 3 Complex viscosity as a function of frequency of PP, PP1 and PP2 processed at 210 °C for 5 and 60 minutes.

As regard the samples processed 5 minutes, as expected, the PP containing 1% of GnP shows a viscosity higher than that of the pure PP processed in the same conditions, but, by doubling the GnP content, the viscosity further increases slightly only at the lowest values of the frequency (outside experimental error). For the nanocomposite samples the non-Newtonian behaviour is more pronounced than that of the matrix. On increasing the mixing time, the viscosity in the low frequency range strongly decreases clearly suggesting a remarkable degradation that leads to a significant reduction of the molecular weight. The reduction of the viscosity is less pronounced for the nanocomposites. Moreover, the viscosity curve of PP1 processed 60 minutes is higher than that of correspondent PP2 system. These results can be attributed to the better stabilizing effect of GnP at the lowest content but also to the modification of the morphology of nanocomposites as a function of the mixing time.

In order to better understand the effect of the presence of the graphene nanoplatelets on the degradation of these nanocomposites, the dimensionless viscosity as a function of the mixing time is reported in the Fig. 4 for all the investigated samples. The dimensionless viscosity has been evaluated as the ratio of the viscosity at the lowest value of the frequency at the three mixing times (5, 15 and 60 min) divided by that of the sample processed 5 min.

The dimensionless data reported in this figure show similar features than that shown by the dimensionless torque curves. The viscosity strongly decreases with mixing time mainly for the matrix. Moreover, the samples processed at the highest temperature, i.e. 240 °C, after 15 minutes, show a greater viscosity decrease than those processed at 210 °C for the same time. This result can be attributed to the higher processing temperature that accelerates the degradative phenomena. Indeed, as reported in literature an higher processing temperature can lead to an abrupt degradation process [36]. The stabilizing effect to the thermal degradation of GnP is again better for the sample with the lowest content of nanoplatelets.

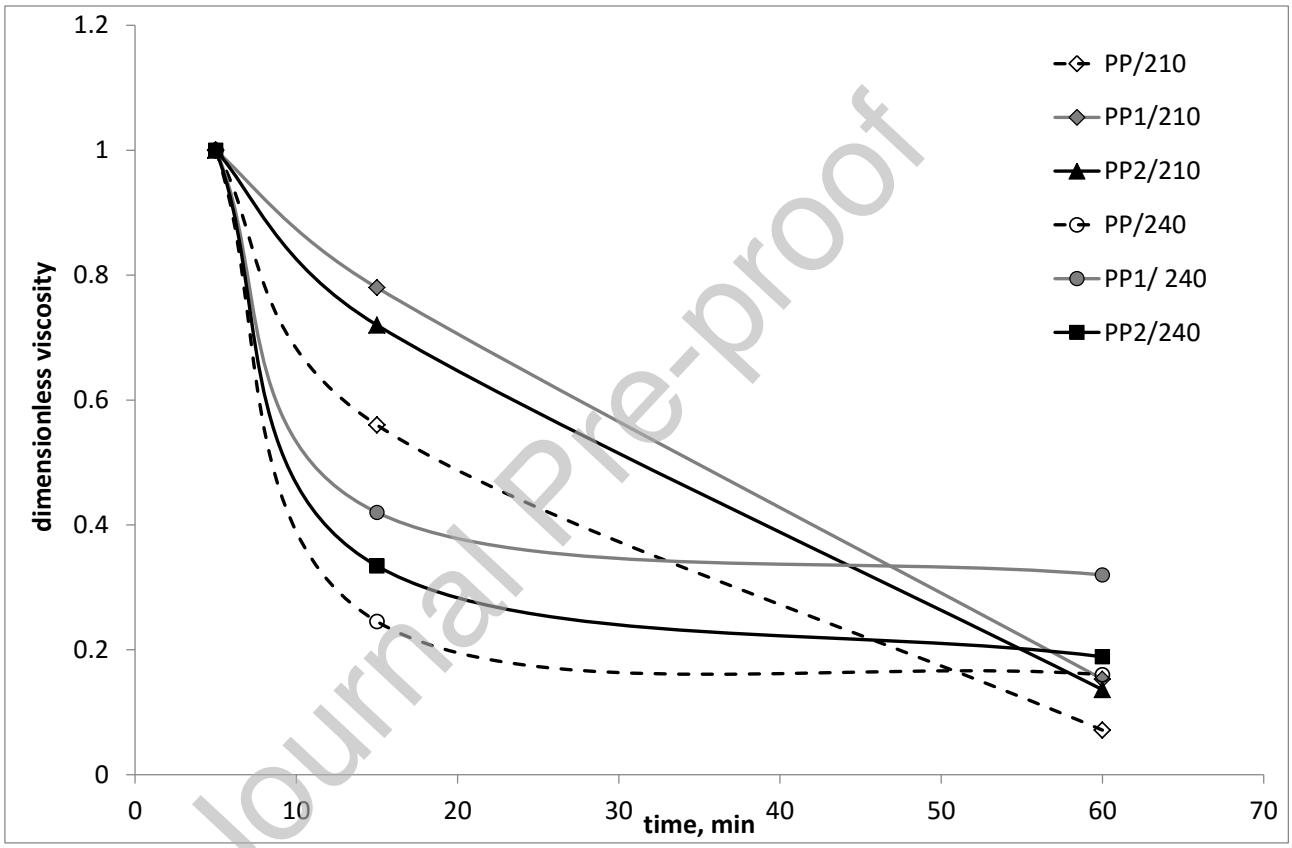

Fig. 4 Dimensionless Viscosity at 0.1 rad/s as a function of the mixing time for all the investigated samples.

In Fig. 5 the same data relative to the nanocomposite samples reported in the figure 4 have been divided by the values of the pure matrix processed at the same temperature. As already done with the curves of the torque, in this way it is possible to remove the degradation of the matrix and observe only the effect of the presence of the graphene.

All the curves present values larger than 1 and this confirms the previous data on the torque and put in evidence the protective effect of the presence of the GnP nanoplatelets on the degradation of the PP matrix. Moreover, it is evident that the lowest content of GnP is more protective but also the nanocomposite with 2% of GnP shows a better resistance to the degradative phenomena than the PP matrix.

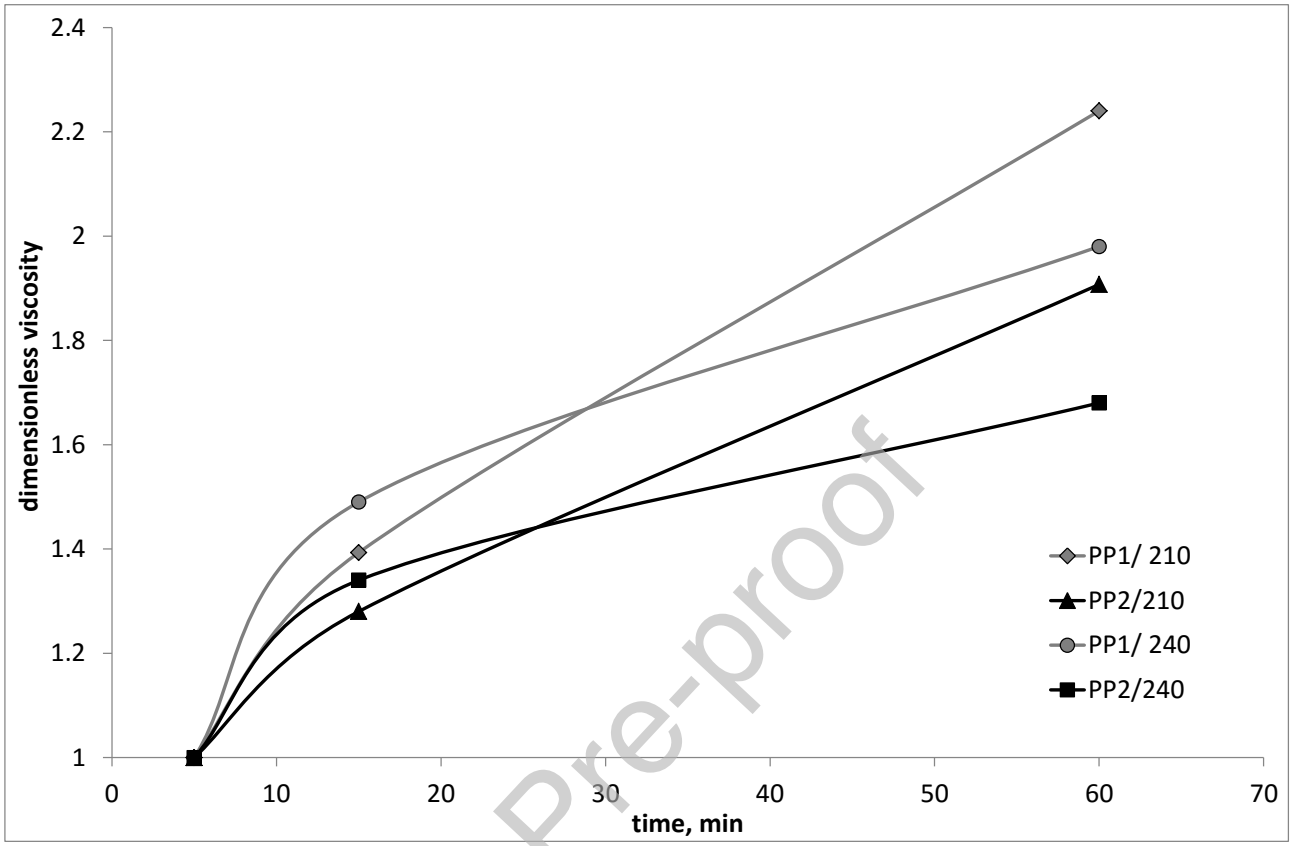

Fig. 5 Dimensionless viscosity at 0,1 s^{-1} as a function of the processing time for the nanocomposite samples divided that of the matrix.

As reported in literature, melt compounding PP in presence of air can lead both to thermo-mechanical and thermo-oxidative degradation of the polymer matrix [35,37,38]. Thermo-oxidative degradation of PP leads to the formation of different oxidation products that can be monitored by FTIR analyses. The generally accepted mechanism is well known and provides that tertiary hydroperoxides are the primary oxidation products, whereas the formation of secondary hydroperoxides is significantly slower. The main oxidation products resulting from the decomposition of hydroperoxides are alcohols, ketones, aldehydes and macroalkyl radicals. The primary chain end macroalkyl radical is further oxidized to an aldehyde. Small amounts of primary alcohols may also be formed. The oxidation of the secondary chain end macroalkyl radical yields a ketone [39]. In Fig. 6 the FTIR spectra of the hydroxyl region (Fig. 6a, and 6c) and of the carbonyl region (Fig. 6b and 6d) for the samples processed 5 and 60 min respectively at 210 °C and at 240 °C are reported. As expected, the spectrum of PP in hydroxyl region show a strong increase of a broad peak centred at about 3350-3400 cm^{-1} on increasing the mixing time. It can be associated to the increase of species containing the –OH group such as hydroperoxides and alcohols [40]. The

carbonyl region of PP processed 60 minutes clearly exhibits the presence of some intense absorption bands. In particular the peak at 1715 cm^{-1} can be associated to the formation of ketones whereas the band at 1740 cm^{-1} is associated to peracids[41]. Moreover, the band at 1650 cm^{-1} is associated at –C=C– double bonds [38,39]

The spectra in both the regions put in evidence that the nanocomposites show the same absorption bands above described for pure matrix, but PP clearly shows the higher increase of the absorption bands both in the hydroxyl and carbonyl regions, while the nanocomposite with a content of 1% of GnP shows the lowest values of the absorptions peaks. These data confirm the more pronounced degradation of the matrix and the stabilizing effect of the GnP especially at the lowest content. Moreover, higher processing temperature gives rise to an increase of the intensity of the absorption bands associated to the above described oxidation products as already reported in literature [42].

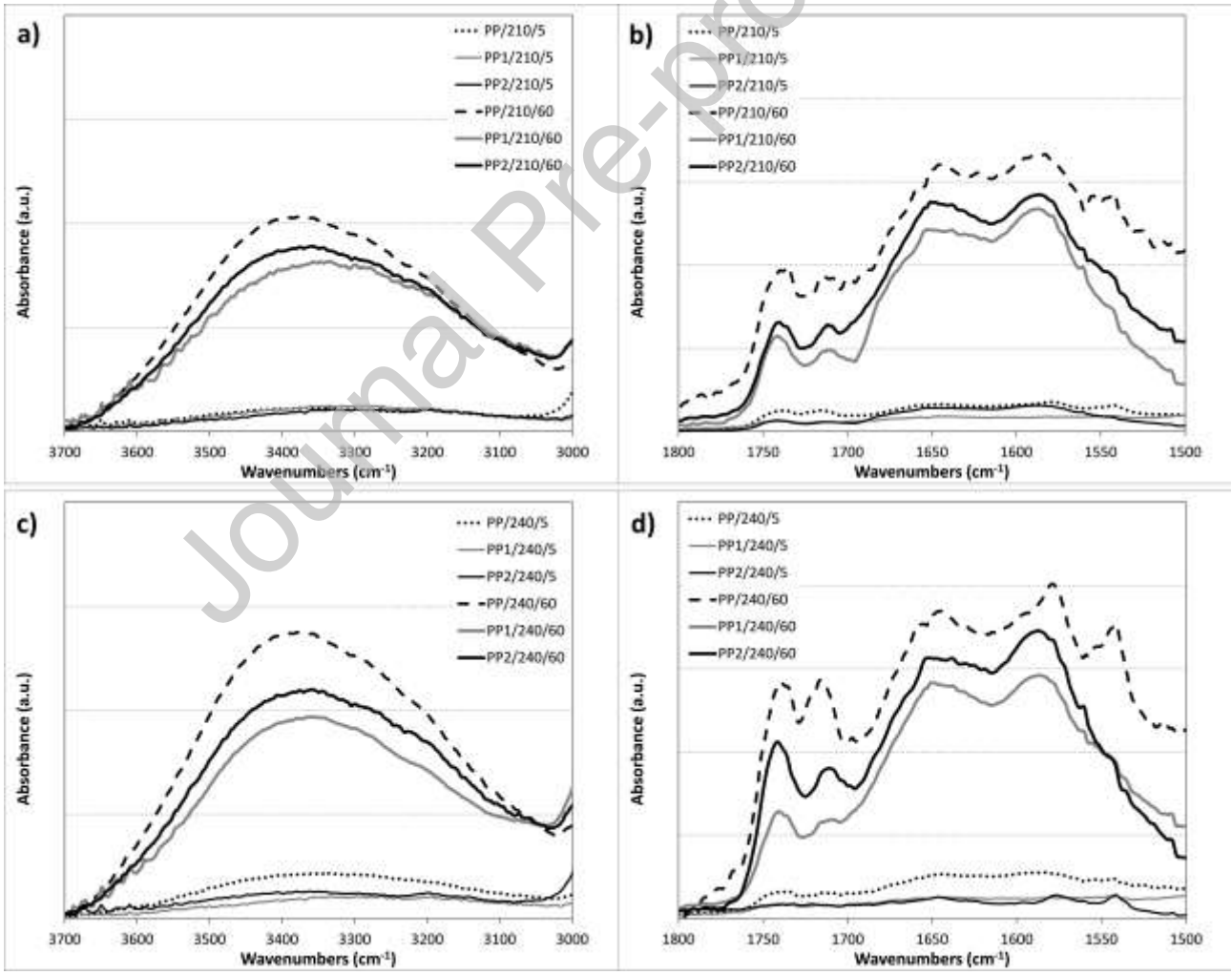

Fig. 6 FTIR spectra at different processing times of the hydroxyl region and of the carbonyl region for samples processed at 210 °C (6a and 6b) and at 240 °C (6c and 6d).

The mechanical properties, elastic modulus (E), tensile strength (TS) and elongation at break (EB), of all the samples are reported in Tab. 2.

Tab. 2 Mechanical properties, elastic modulus (E), tensile strength (TS) and elongation at break (EB), of all the investigated samples

	E, MPa			**T.S, MPa**			**EB, %**		
time, min	**5**	**15**	**60**	**5**	**15**	**60**	**5**	**15**	**60**
PP/210	490 ±13	508 ±11	554 ±19	22.5 ±1.3	18.9 ±1.2	17.8 ±1.3	628 ±20	330 ±11	41 ±3
PP1/210	658 ±16	676 ±12	680 ±18	17.7 ±1.4	16.3 ±1.1	15.6 ±1.4	387 ±10	277 ±7	87 ±4
PP2/210	726 ±17	751 ±18	752 ±13	15.8 ±1.6	14.1 ±1.1	13.5 ±1.1	313 ±9	180 ±9	38 ±3
PP/240	485 ±14	518 ±13	579 ±11	22.1 ±1.3	18.2 ±1.4	16.8 ±1.3	610 ±19	220 ±8	15 ±2
PP1/240	648 ±18	667 ±14	675 ±16	16.5 ±1.2	14.8 ±1.2	14.1 ±1.2	260 ±11	158 ±7	50 ±3
PP2/240	717 ±19	749 ±15	760 ±16	15.1 ±1.1	13.2 ±1.3	12.3 ±1.0	181 ±8	86 ±5	15 ±2

The presence of the GnP improves the rigidity of the PP matrix as the elastic modulus increases with increasing the nanoparticles content. However, while the increase of the elastic modulus of the matrix for the samples prepared with the shortest processing time is about 30% with 1% of GnP, the nanocomposite with 2% of GnP shows moduli of less than 15% higher than those of the nanocomposite samples with 1%. The increase is, then, non linear with the GnP content and this means that the mechanisms which give rise to the change of the mechanical properties depend on the filler content, but also on the dispersion and on the possible agglomeration of the nanoparticles. Indeed, as shown by SEM micrographs of nanocomposites processed at 210 °C for 5 minutes reported in Fig. 7, PP incorporating 1% of GnP exhibited a better dispersion and a lower dimension of agglomerates.

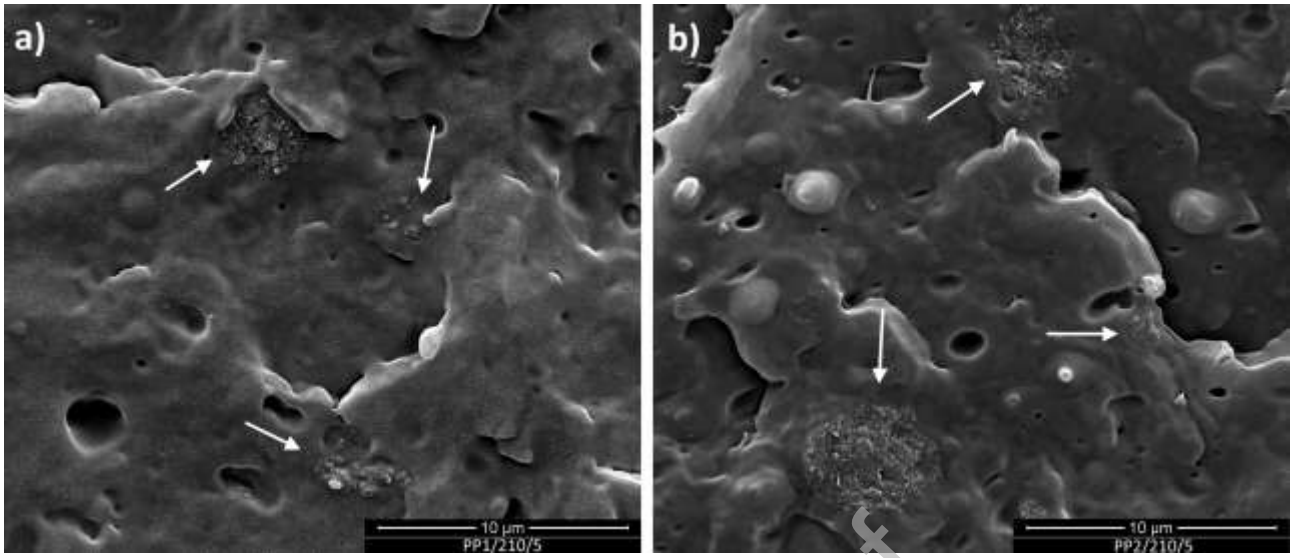

Fig. 7 SEM micrographs of nanocomposites processed at 210 °C for 5 minutes: (a) PP1 and (b) PP2.

The properties at break decrease with increasing the GnP content. The decrease of the tensile strength is due to reduction of the elongation at break. Nevertheless, despite the presence of a very high number of nanoplatelets, the materials are ductile and the elongation at break remains relatively elevated like the tensile strength. The decrease of the tensile strength is, of course, due to the reduction of the elongation at break which causes a premature breaking of the specimen.

As for the effect of the processing conditions, the elastic modulus increases with the processing time and the processing temperature, while tensile strength and elongation at break decreases (see Fig. 8). All these last modifications can be correlated with the decrease of the molecular weight and the contemporary increase of the crystallinity degree due to increased mobility of the shorter chain length [10,26]. Both changes in the molecular structure and in the morphology lead to a drastic decrease of the elongation at break.

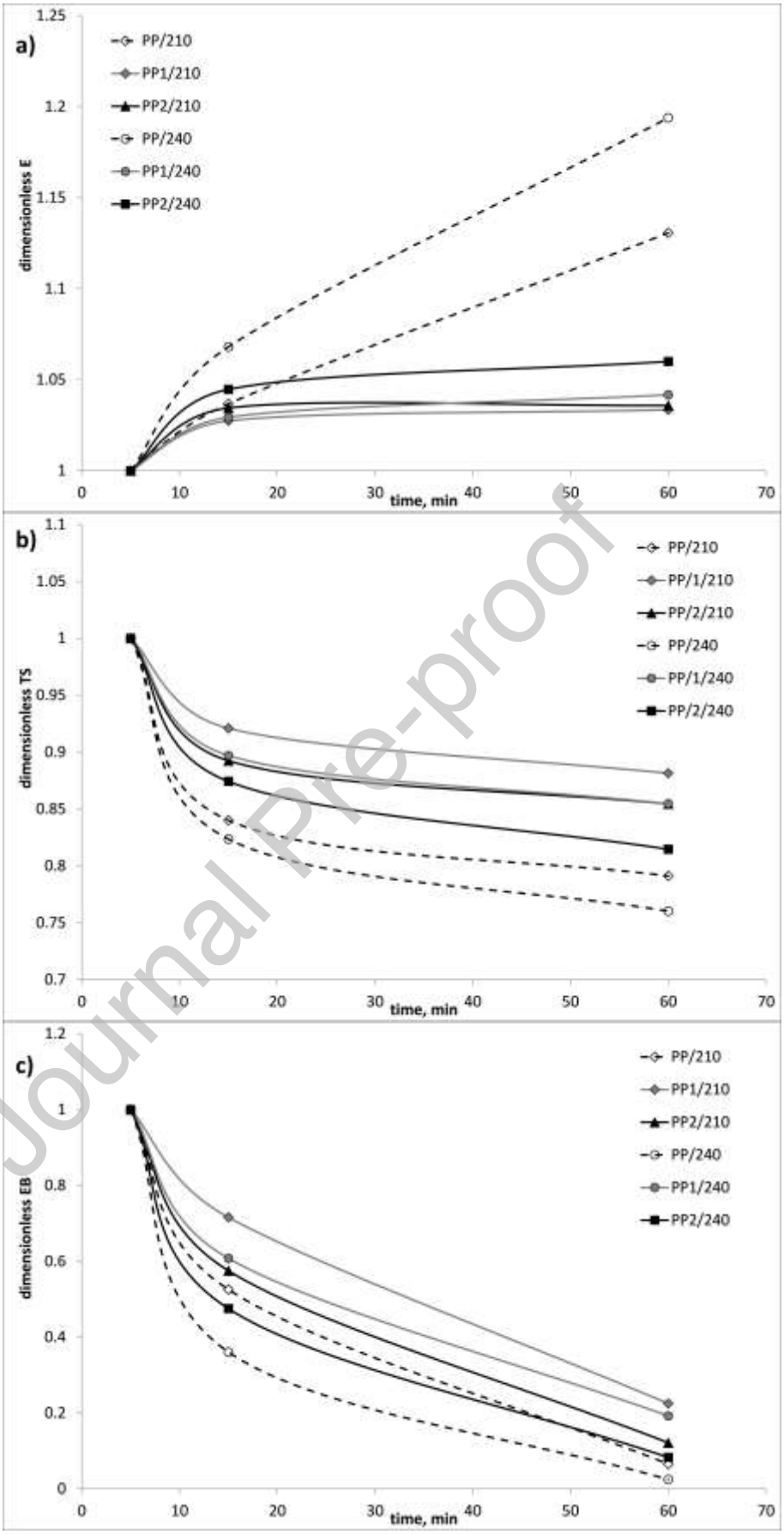

Fig. 8 Dimensionless values of the Elastic modulus (a), tensile strength (b) and elongation at break (c) of all investigated samples.

The values of the enthalpy of fusion and crystallinity degree of all the samples are reported in Tab. 3. The presence of the nanoparticles slightly increases the crystallinity degree of the matrix, but a slightly larger increase of crystallinity can be noticed as a function of the processing conditions. Moreover, as shown in Fig. 9 where the dimensionless values of the crystallinity degree is reported as a function of the processing time, the neat matrix exhibits at both the temperatures a slightly larger increase of crystallinity compared with the nanocomposite samples.

Tab. 3 Enthalpy of fusion and crystallinity degree of all the samples.

	ΔH_m, J/g			**X_c, %**		
time, min	**5**	**15**	**60**	**5**	**15**	**60**
PP/210	64.9 ± 0.2	66.6 ± 0.3	67.3 ± 0.3	31.1 ± 0.10	31.9 ± 0.14	32.2 ± 0.14
PP1/210	66.3 ± 0.3	67.5 ± 0.2	68.0 ± 0.2	32,0 ± 0.14	32,6 ± 0.10	32.9 ± 0.10
PP2/210	64.5 ± 0.2	65.8 ± 0.2	66.4 ± 0.3	31.5 ± 0.10	32.1 ± 0.10	32.4 ± 0.14
PP/240	67.5 ± 0.3	70.9 ± 0.4	72.3 ± 0.4	32.3 ± 0.14	33.9 ± 0.19	34.6 ± 0.19
PP1/240	67.5 ± 0.3	69.1 ± 0.2	69.8 ± 0.2	32.6 ± 0.14	33.4 ± 0.10	33.7 ± 0.10
PP2/240	67.2 ± 0.2	69.1 ± 0.2	69.9 ± 0.2	32.8 ± 0.10	33.7 ± 0.10	34.1 ± 0.10

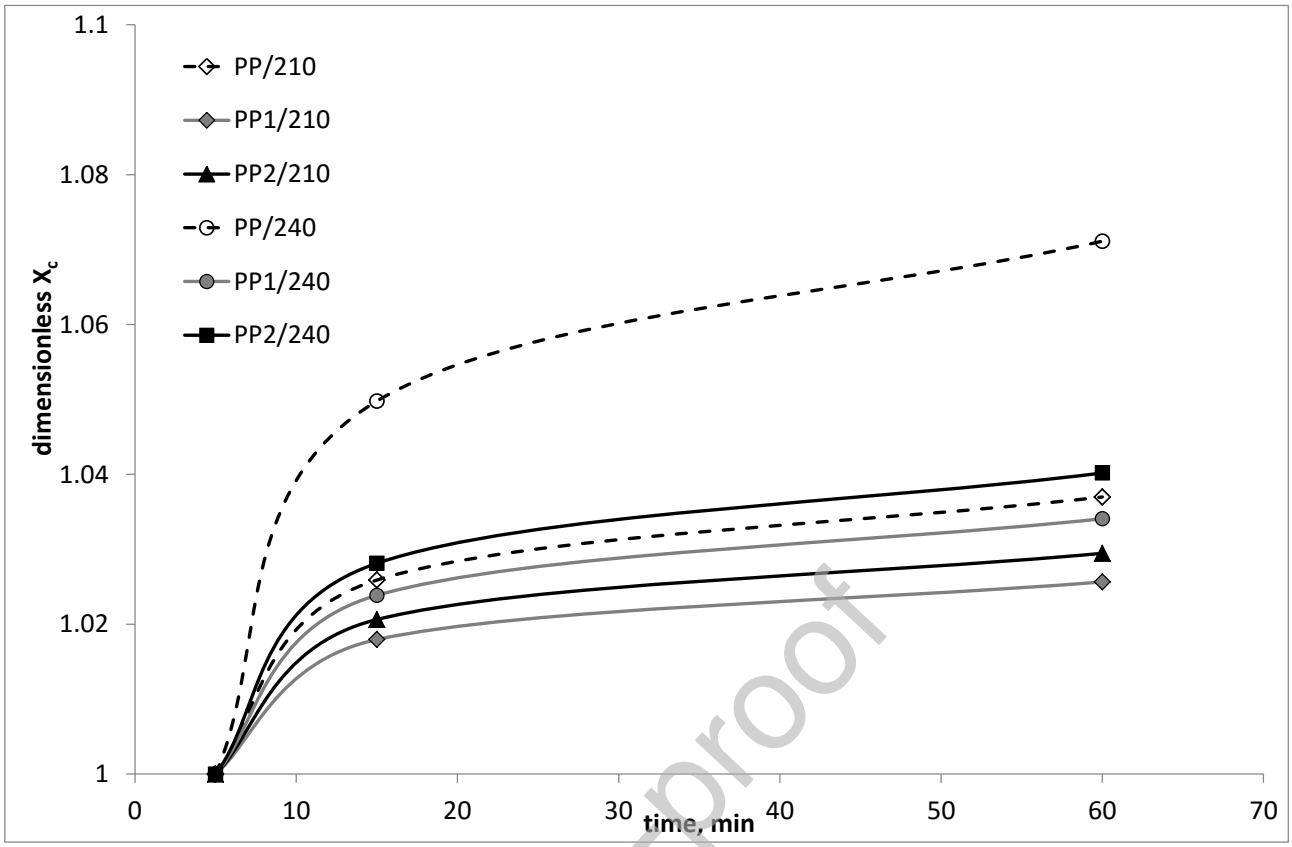

Fig. 9 Dimensionless crystallinity degree as a function of the processing time for all the investigated samples.

From these curves it is evident that the crystallinity increases with increasing the processing time and with the increase of processing temperature. These data are in agreement with viscosity data above reported. The increase of crystallinity is responsible for the increase of the elastic modulus. The minor effect on the variation of crystallinity as a function of the processing time is again shown by the nanocomposite with 1% of GnP, while the matrix exhibits a larger variation.

All the previous experimental data suggest that the presence of the graphene nanoplatelets improves the thermo-mechanical resistance to the polymer matrix, but this effect does not improve with the GnP content as the degradative phenomena are more relevant for the system with a content of 2% of GnP. However, even in this case, the nanocomposite shows a better resistance to the thermo-mechanical and thermo-oxidative degradation than the pure matrix.

A better resistance to the thermal degradation of nanocomposites with graphene has been already reported in the literature as the weight loss shifted to higher temperature in presence of graphene[28,29]. This behaviour has been correlated with an effective gas barrier of the GnP which reduce the permeability of the PP matrix to oxygen molecules. The depletion of oxygen causes a beneficial effect on the thermo-oxidative degradation of the matrix.

In these tests the same interpretation can be taken into account and explain the protective behaviour of the GnP. In compounding tests, however, this effect seems more relevant as the flow increases the penetration and the mixing of oxygen in the melt. However, this interpretation does not explain the better stabilizing effect at the lower content of GnP. Indeed, increasing the content of the GnP nanoplatelets, the barrier effect due to the presence of the nanoplatelets should be better. In Fig. 10 the SEM micrographs of the two nanocomposites processed at 240 °C for 5 and 60 min are reported. The GnP nanoplatelets are agglomerated in small agglomerates of about 2.1 µm for the PP1 sample and of about 4.1 µm for PP2 sample processed 5 min. These agglomerates become smaller after 60 min of mixing because of the shear stress applied for this long time.

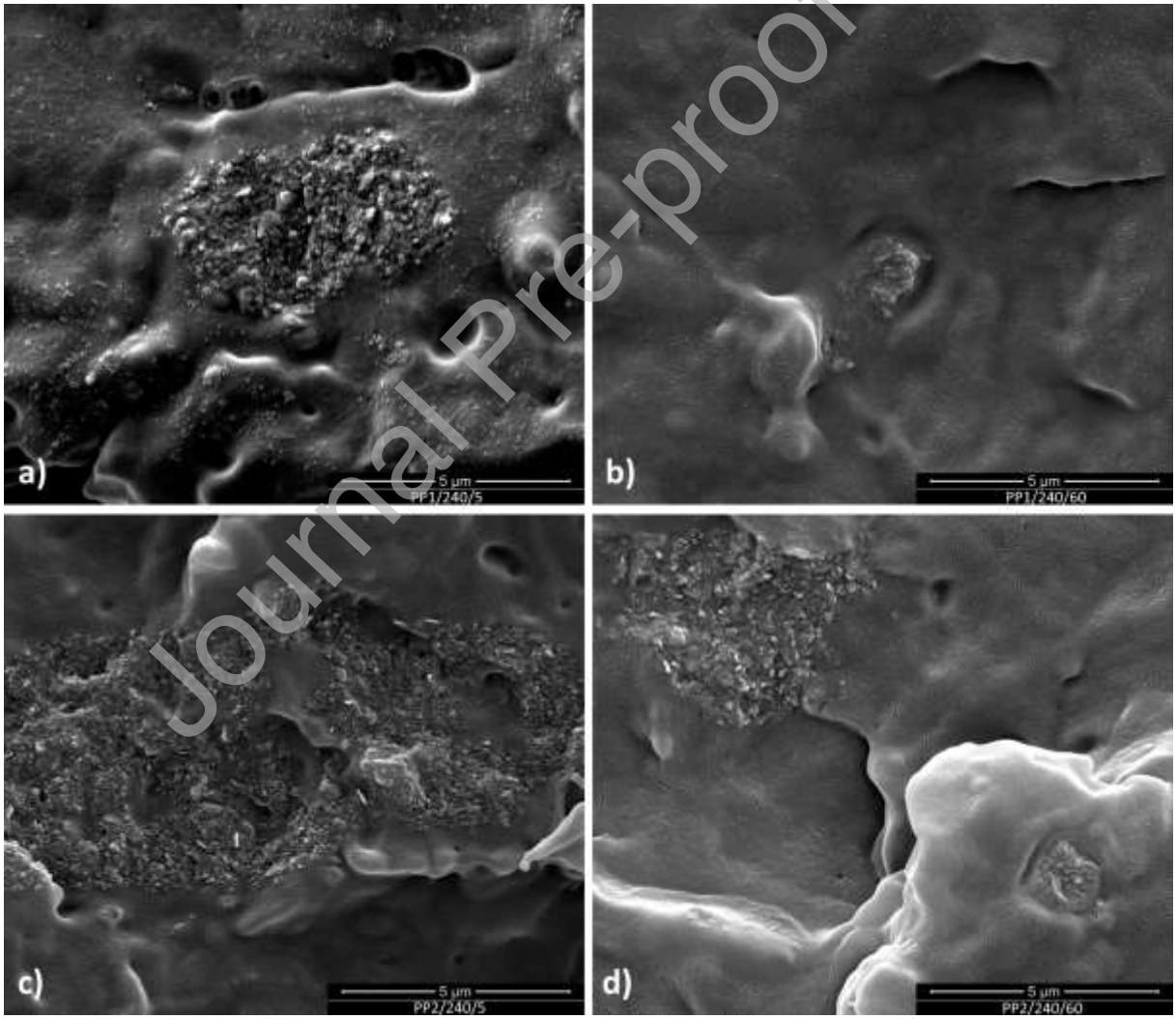

Fig. 10 SEM micrographs of nanocomposites processed at 240 °C for 5 and 60 minutes: (a) PP1/240/5, (b) PP1/240/60, (c) PP2/240/5 and (d) PP2/240/60.

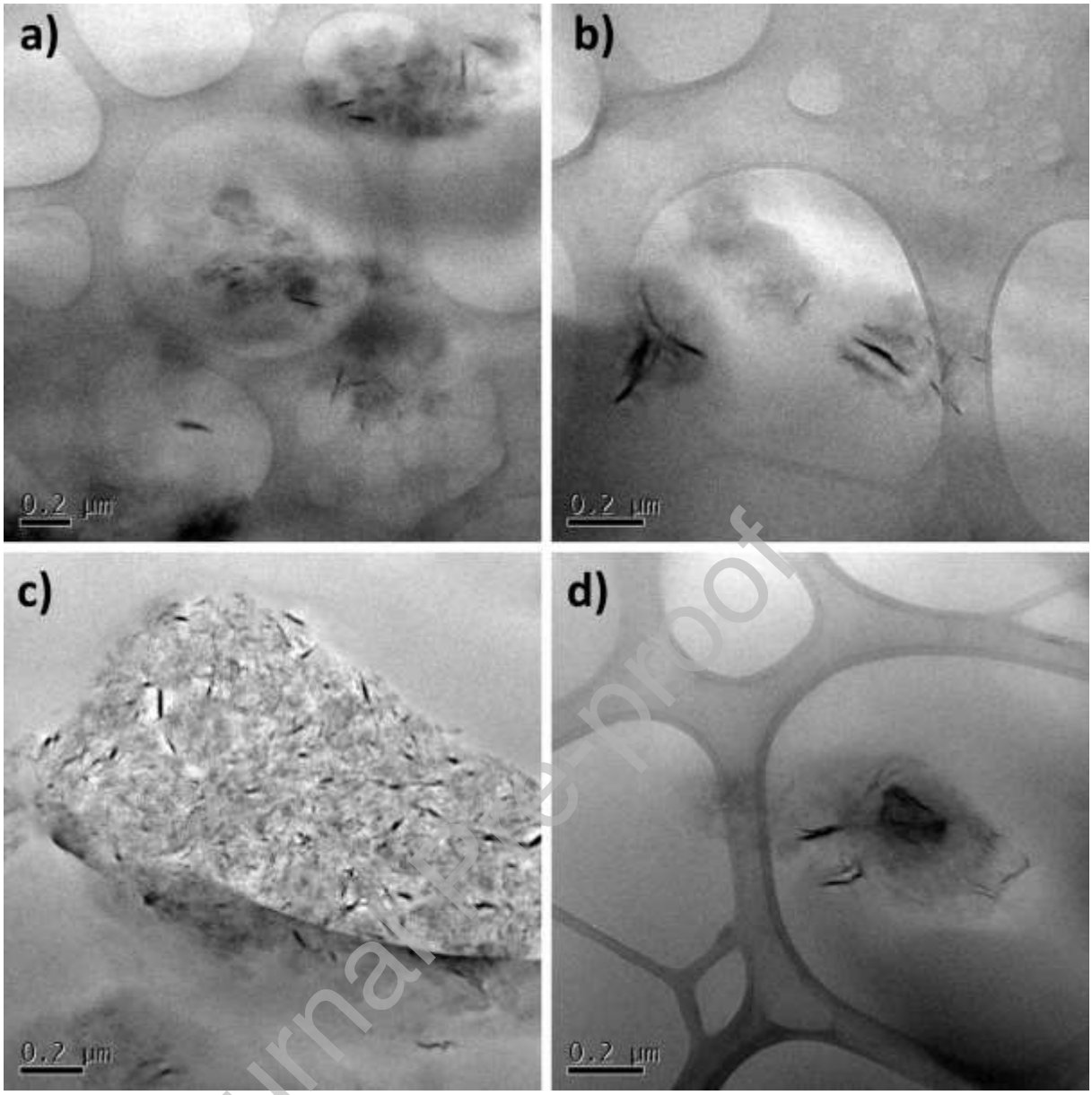

Fig. 11 TEM images of nanocomposites processed at 240 °C for 5 and 60 minutes: (a) PP1/240/5, (b) PP1/240/60, (c) PP2/240/5 and (d) PP2/240/60.

This phenomenon is corroborated at nanoscale by TEM images reported in Fig. 11 where two nanocomposites processed at 240 °C for 5 and 60 min are reported. Indeed, the images show that a fairly good level of dispersion at nano-scale was achieved during the compounding for PP1, i.e. the typical flake morphology of GnP is evident, although single layers are not present but agglomerates, each comprised of several GnP platelets. Moreover, on increasing the amount of incorporated GnP, the dimension of aggregates increases. The smaller sizes of the GnP at lower content can be considered responsible for the better stabilizing effect of the nanofiller as the contact surface – and then the barrier to the oxygen - increases with the smaller size of the

nanoplatelets. A similar effect has been already reported in the literature where the reinforcing effect of the GnP nanoplatelets on the mechanical properties of fibers made of the same nanocomposite is better at lower content of GnP [12]. It has been demonstrated that the surface area was higher for the sample with a lower content of GnP due to the agglomeration of the nanoplatelets in the sample with high content of GnP.

CONCLUSIONS

During processing the morphology and the molecular structure of molten polymer can be modified due to the application of mechanical and thermal stress. The level of degradation undergone depends, of course, on the level of the thermo-mechanical stress but also on the nature and molecular structure of the polymers and on the availability of oxygen during the processing. For composite polymeric systems the level of degradation depends also on the type of the filler and on its interactions with the polymer matrix. In this work it has been put in evidence the effect of the graphene nanoplatelets on the thermo-mechanical degradation of the polypropylene during compounding in presence of oxigen. The presence of the GnP slows down the degradation of the polypropylene but this stabilizing effect does not increase with the GnP content and moreover is better at the lower GnP content investigated.

The first feature is in agreement with previous studies and is due to the barrier effect of the graphene nanoplatelets that hinders the penetration of the oxygen reducing, then, the oxidation of the matrix. As for the second effect, it has been interpreted considering the agglomeration of the graphene nanoplatelets with increasing the GnP content and this agglomeration reduces the surface are with respect to the samples with lower content of GnP. Of course, the reduced surface means to give rise to a reduced barrier effect of the GnP.

Acknowledgment

This work has been financially supported by the project PON03PE_00206_3 (NanoBioMat)

Data availability

The raw/processed data required to reproduce these findings cannot be shared at this time as the data also forms part of an ongoing study.

Credit Author Statement

Luigi Botta: Formal analysis, Data Curation, Writing - Original Draft, Writing - Review & Editing, Visualization

Francesco Paolo La Mantia: Conceptualization, Methodology, Supervision, Funding acquisition, Data curation, Writing- Original Draft.

Manuela Ceraulo: Investigation, Validation, Formal analysis.

***Maria Chiara Mistretta**:* Investigation, Validation, Formal analysis.

Declaration of interests

The authors declare that they have no known competing financial interests or personal relationships that could have appeared to influence the work reported in this paper.

References

[1] H. Kim, A.A. Abdala, C.W. MacOsko, Graphene/polymer nanocomposites, Macromolecules. 43 (2010) 6515–6530. doi:10.1021/ma100572e.

[2] B. Li, W.H. Zhong, Review on polymer/graphite nanoplatelet nanocomposites, J. Mater. Sci. 46 (2011) 5595–5614. doi:10.1007/s10853-011-5572-y.

[3] M.J. Allen, V.C. Tung, R.B. Kaner, Honeycomb Carbon: A Review of Graphene, Chem. Rev. 110 (2010) 132–145. doi:10.1021/cr900070d.

[4] W. Choi, I. Lahiri, R. Seelaboyina, Y.S. Kang, Synthesis of Graphene and Its Applications: A Review, Crit. Rev. Solid State Mater. Sci. 35 (2010) 52–71. doi:10.1080/10408430903505036.

[5] T. Kuilla, S. Bhadra, D. Yao, N.H. Kim, S. Bose, J.H. Lee, Recent advances in graphene based polymer composites, Prog. Polym. Sci. 35 (2010) 1350–1375. doi:10.1016/j.progpolymsci.2010.07.005.

[6] H. Norazlina, Y. Kamal, Graphene modifications in polylactic acid nanocomposites: a review, Polym. Bull. 72 (2015) 931–961. doi:10.1007/s00289-015-1308-5.

[7] R. Scaffaro, L. Botta, A. Maio, M. Mistretta, F. La Mantia, Effect of Graphene Nanoplatelets on the Physical and Antimicrobial Properties of Biopolymer-Based Nanocomposites, Materials (Basel). 9 (2016) 351. doi:10.3390/ma9050351.

[8] R. Scaffaro, L. Botta, A. Maio, G. Gallo, PLA graphene nanoplatelets nanocomposites: Physical properties and release kinetics of an antimicrobial agent, Compos. Part B Eng. 109 (2017) 138–146. doi:10.1016/j.compositesb.2016.10.058.

[9] C. Gonçalves, I. Gonçalves, F. Magalhães, A. Pinto, Poly(lactic acid) Composites Containing Carbon-Based Nanomaterials: A Review, Polymers (Basel). 9 (2017) 269. doi:10.3390/polym9070269.

[10] L. Botta, R. Scaffaro, F. Sutera, M.C. Mistretta, Reprocessing of PLA/graphene nanoplatelets nanocomposites, Polymers (Basel). 10 (2017) 18. doi:10.3390/polym10010018.

[11] K. Kalaitzidou, H. Fukushima, L.T. Drzal, Mechanical properties and morphological characterization of exfoliated graphite–polypropylene nanocomposites, Compos. Part A Appl. Sci. Manuf. 38 (2007) 1675–1682. doi:10.1016/j.compositesa.2007.02.003.

[12] F.P. La Mantia, M. Ceraulo, M.C. Mistretta, L. Botta, Effect of the elongational flow on morphology and properties of polypropylene/graphene nanoplatelets nanocomposites, Polym. Test. 71 (2018) 10–17. doi:10.1016/j.polymertesting.2018.08.016.

[13] M.C. Mistretta, L. Botta, A.D. Vinci, M. Ceraulo, F.P. La Mantia, Photo-oxidation of polypropylene/graphene nanoplatelets composites, Polym. Degrad. Stab. 160 (2019) 35–43. doi:10.1016/j.polymdegradstab.2018.12.003.

[14] V.B. Mohan, K. Lau, D. Hui, D. Bhattacharyya, Graphene-based materials and their composites: A review on production, applications and product limitations, Compos. Part B Eng. 142 (2018) 200–220. doi:10.1016/j.compositesb.2018.01.013.
[15] E. Cunha, M.C. Paiva, L. Hilliou, J.A. Covas, Tracking the progression of dispersion of graphite nanoplates in a polypropylene matrix by melt mixing, Polym. Compos. 38 (2017) 947–954. doi:10.1002/pc.23657.
[16] R. Santos, S. Mould, P. Formánek, M. Paiva, J. Covas, Effects of Particle Size and Surface Chemistry on the Dispersion of Graphite Nanoplates in Polypropylene Composites, Polymers (Basel). 10 (2018) 222. doi:10.3390/polym10020222.
[17] P. Rodrigues, R.M. Santos, M.C. Paiva, J.A. Covas, Development of Dispersion during Compounding and Extrusion of Polypropylene/Graphite Nanoplates Composites, Int. Polym. Process. 32 (2017) 614–622. doi:10.3139/217.3485.
[18] M. Liebscher, J. Domurath, M. Saphiannikova, M.T. Müller, G. Heinrich, P. Pötschke, Dispersion of graphite nanoplates in melt mixed PC/SAN polymer blends and its influence on rheological and electrical properties, Polymer (Guildf). (2020) 122577. doi:10.1016/j.polymer.2020.122577.
[19] W. Gianelli, G. Camino, N.T. Dintcheva, S. Lo Verso, F.P. La Mantia, EVA-Montmorillonite Nanocomposites: Effect of Processing Conditions, Macromol. Mater. Eng. 289 (2004) 238–244. doi:10.1002/mame.200300267.
[20] R. Scaffaro, L. Botta, E. Passaglia, W. Oberhauser, M. Frediani, L. Di Landro, Comparison of different processing methods to prepare poly(lactid acid)-hydrotalcite composites, Polym. Eng. Sci. 54 (2014) 1804–1810. doi:10.1002/pen.23724.
[21] N.T. Dintcheva, F.P. La Mantia, Thermo-Mechanical Degradation of LDPE-Based Nanocomposites, Macromol. Mater. Eng. 292 (2007) 855–862. doi:10.1002/mame.200700075.
[22] M.C. Mistretta, M. Morreale, F.P. La Mantia, Thermomechanical degradation of polyethylene/polyamide 6 blend-clay nanocomposites, Polym. Degrad. Stab. 99 (2014) 61–67. doi:10.1016/j.polymdegradstab.2013.12.009.
[23] R. Scaffaro, L. Botta, M.C. Mistretta, F.P. La Mantia, Processing – morphology – property relationships of polyamide 6/polyethylene blend–clay nanocomposites, Express Polym. Lett. 7 (2013) 873–884. doi:10.3144/expresspolymlett.2013.84.
[24] F.P. La Mantia, M.C. Mistretta, M. Morreale, Recycling and Thermomechanical Degradation of LDPE/Modified Clay Nanocomposites, Macromol. Mater. Eng. 299 (2014) 96–103. doi:10.1002/mame.201200449.
[25] F.P. La Mantia, M.C. Mistretta, R. Scaffaro, L. Botta, M. Ceraulo, Processing and characterization of highly oriented fibres of biodegradable nanocomposites, Compos. Part B Eng. 78 (2015) 1–7. doi:10.1016/j.compositesb.2015.03.054.
[26] R. Scaffaro, F. Sutera, M.C. Mistretta, L. Botta, F.P. La Mantia, Structure-properties relationships in melt reprocessed PLA/hydrotalcites nanocomposites, Express Polym. Lett. 11 (2017). doi:10.3144/expresspolymlett.2017.53.
[27] F.P. La Mantia, M.C. Mistretta, S. Palermo, E. Koci, M. Ceraulo, Thermomechanical degradation of PLA-based nanobiocomposite, Polym. Adv. Technol. 27 (2016) 308–313. doi:10.1002/pat.3637.
[28] G. Gedler, M. Antunes, V. Realinho, J.I. Velasco, Thermal stability of polycarbonate-graphene nanocomposite foams, Polym. Degrad. Stab. 97 (2012) 1297–1304. doi:10.1016/j.polymdegradstab.2012.05.027.
[29] M. Li, Y.G. Jeong, Poly(ethylene terephthalate)/exfoliated graphite nanocomposites with improved thermal stability, mechanical and electrical properties, Compos. Part A Appl. Sci. Manuf. 42 (2011) 560–566. doi:10.1016/j.compositesa.2011.01.015.
[30] L. Gan, S. Shang, C.W.M. Yuen, S. Jiang, N.M. Luo, Facile preparation of graphene nanoribbon filled silicone rubber nanocomposite with improved thermal and mechanical

properties, Compos. Part B Eng. 69 (2015) 237–242. doi:10.1016/j.compositesb.2014.10.019.

[31] Y. Lee, D. Kim, J. Seo, H. Han, S.B. Khan, Preparation and characterization of poly(propylene carbonate)/exfoliated graphite nanocomposite films with improved thermal stability, mechanical properties and barrier properties, Polym. Int. 62 (2013) 1386–1394. doi:10.1002/pi.4434.

[32] S.M.A. Jafari, R. Khajavi, V. Goodarzi, M.R. Kalaee, H.A. Khonakdar, Development of degradable poly(ethylene terephthalate)- based nanocomposites with the aid of polylactic acid and graphenic materials: Thermal, thermo- oxidative and hydrolytic degradation characteristics, J. Appl. Polym. Sci. 137 (2020) 48466. doi:10.1002/app.48466.

[33] K. Kalaitzidou, H. Fukushima, L.T. Drzal, Mechanical properties and morphological characterization of exfoliated graphite–polypropylene nanocomposites, Compos. Part A Appl. Sci. Manuf. 38 (2007) 1675–1682. doi:10.1016/j.compositesa.2007.02.003.

[34] M. Gahleitner, J. Wolfschwenger, C. Bachner, K. Bernreitner, W. Neiβl, Crystallinity and mechanical properties of PP-homopolymers as influenced by molecular structure and nucleation, J. Appl. Polym. Sci. 61 (1996) 649–657. doi:10.1002/(SICI)1097-4628(19960725)61:4<649::AID-APP8>3.0.CO;2-L.

[35] W.R. Waldman, M.A. De Paoli, Thermo-mechanical degradation of polypropylene, low-density polyethylene and their 1:1 blend, Polym. Degrad. Stab. 60 (1998) 301–308. doi:10.1016/S0141-3910(97)00083-9.

[36] H.M. da Costa, V.D. Ramos, M.C.G. Rocha, Rheological properties of polypropylene during multiple extrusion, Polym. Test. 24 (2005) 86–93. doi:10.1016/j.polymertesting.2004.06.006.

[37] P. Gijsman, Review on the thermo-oxidative degradation of polymers during processing and in service, E-Polymers. 8 (2008) 1–34. doi:10.1515/epoly.2008.8.1.727.

[38] H. Hinsken, S. Moss, J.-R. Pauquet, H. Zweifel, Degradation of polyolefins during melt processing, Polym. Degrad. Stab. 34 (1991) 279–293. doi:10.1016/0141-3910(91)90123-9.

[39] R. Gensler, C.J.. Plummer, H.-H. Kausch, E. Kramer, J.-R. Pauquet, H. Zweifel, Thermo-oxidative degradation of isotactic polypropylene at high temperatures: phenolic antioxidants versus HAS, Polym. Degrad. Stab. 67 (2000) 195–208. doi:10.1016/S0141-3910(99)00113-5.

[40] J. Lacoste, D. Vaillant, S. Chmela, GAMMA-, PHOTO- AND THERMALLY-INITIATED OXIDATION OF POLYOLEFINES USED IN PACKAGING, J. Polym. Eng. 15 (1995) 139–152. doi:10.1515/POLYENG.1995.15.1-2.139.

[41] S. de Goede, R. Brüll, H. Pasch, N. Marshall, Monitoring thermo-oxidative degradation of polypropylene by CRYSTAF and SEC-FTIR, Macromol. Symp. 193 (2003) 35–44. doi:10.1002/masy.200390062.

[42] L.A. Pinheiro, M.A. Chinelatto, S.V. Canevarolo, The role of chain scission and chain branching in high density polyethylene during thermo-mechanical degradation, Polym. Degrad. Stab. 86 (2004) 445–453. doi:10.1016/j.polymdegradstab.2004.05.016.